Residual Stress-induced Crack-tip Constraint: A Parametric Study

X.B. Ren[1, a], Z.L. Zhang[1, b] and B. Nyhus[2, c]

[1] Department of Structural Engineering, Norwegian University of Science and Technology (NTNU), N-7491 Trondheim, Norway

[2] SINTEF Materials and Chemistry, N-7465 Trondheim, Norway

[a]xiaobo.ren@ntnu.no, [b]zhiliang.zhang@ntnu.no, [c] bard.nyhus@sintef.no

Keywords: Residual stress, Crack-tip constraint, Cleavage fracture

Abstract. In this work, the effect of residual stress on the crack-tip constraint is studied under mode I, plane strain conditions. The modified boundary layer simulations are performed with the remote boundary conditions controlled by the stress intensity factor K and *T-stress*. The eigenstrain method was used to introduce a two-dimensional residual stress field near the crack-tip. It is found that the residual stress field can significantly elevate the crack-tip constraint and thus enhance the probability for cleavage fracture. The constraint parameter R is defined to characterize the residual stress-induced crack-tip constraint. Results also show that the R value decreases with the increase in the external load. The effect of residual stress on the crack-tip constraint is smaller for weaker hardening materials. The R value was also calculated for different geometry constraint level, and the results indicate that the R becomes smaller for the case with higher geometry constraint.

Introduction

Residual stresses are inevitable for most mechanical or thermal operations used in processing the engineering materials. Residual stresses have significant effect on the structure integrity assessment of welded structures. Understanding how the residual stresses affect the crack driving force and the crack-tip constraint is a fundamental problem. The present study concentrates on the residual stress-induced crack-tip constraint.

Constraint in fracture mechanics is a term that is widely used but vaguely defined or understood. In the present context we prefer to understand the level of constraint an indicator of the near-tip stress state, and the constraint is regarded as the factors or conditions which influence the transferability and invalidate the one-to-one relation between the crack driving force and near-tip stress field. There are basically four factors which influence the level of a crack-tip constraint, i.e. the geometry constraint, the mismatch constraint, the prestrain history-induced constraint and the constraint induced by the residual stresses.

Betegón and Hancock [1] suggested a two-parameter framework J-T to characterize the effect of the constraint induced by the geometry in an elastic regime. O'Dowd and Shih [2, 3] developed the J-Q two-parameter theory and gave a precise meaning to the term of constraint caused by the geometry and loading mode. By considering the interface crack as a bi-material system, Zhang et al. carried out a numerical investigation on the near-tip stress field and a parameter M was defined to measure the mismatch constraint [4]. Similar studies have also been carried out for the crack in the middle of weld [5, 6]. Plastic prestrain history in reeled pipes has also been found to influence on the crack-tip constraint [7]. A new constraint parameter P was developed to quantify the prestrain history induced crack-tip constraint by considering single prestrain cycle. Most recently, Liu et al. [8] investigated the residual stress-induced crack-tip constraint by using single notched bending specimen and a one-dimensional residual stress field. They proposed a parameter R to quantify the residual stress-induced constraint.

In this study, a modified boundary layer (MBL) model has been used to investigate the effect of two-dimensional residual stress fields on the crack-tip constraint under mode I, plane strain

conditions. An ideal problem, a larger round cylinder with a round shape weld in the center, was studied (see Fig.1). A rigid analytical surface was placed on the symmetrical line to model the contact of the crack surfaces. The remote boundary of MBL model is controlled by the elastic *K-field* and *T-stress*, and with a crack located at the weld metal. The material property mismatch between the weld metal and the base metal is not considered. The parameter *R*, which is used to quantify the effect of residual stress on the crack-tip constraint, was defined based on the difference in opening stress components between the full stress field and the reference stress field. The results show that the *R* value decreases with the increase in the external loading.

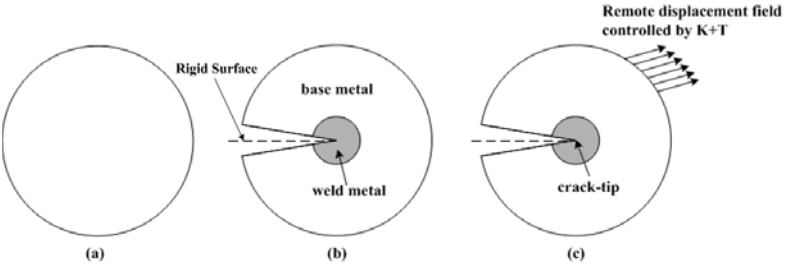

Fig.1. Illustration of the problem. (a) the round cylinder; (b) the round shape weld in the center and one sharp crack is introduced; (c) applied load.

Numerical procedure

The present analyses are carried out for conditions of small-scale yielding. Due to the symmetry about the crack plane only half of the model needs to be analyzed. The MBL model used for this study consists of a weld metal region located in the center of the model and an outer base metal region, and a sharp crack was assumed in the center of weld metal region. The load was applied to the remote edges of the model through a displacement field (*u, v*) controlled by the elastic asymptotic stress field of a plane strain mode I crack:

$$u(r,\theta) = K_I \frac{1+v}{E}\sqrt{\frac{r}{2\pi}}\cos\left(\frac{1}{2}\theta\right)(3-4v-\cos\theta)+T\frac{1-v^2}{E}r\cos\theta$$
$$v(r,\theta) = K_I \frac{1+v}{E}\sqrt{\frac{r}{2\pi}}\sin\left(\frac{1}{2}\theta\right)(3-4v-\cos\theta)-T\frac{v(1+v)}{E}r\sin\theta \quad (1)$$

where $K_I = \sqrt{EJ/1\text{-}v^2}$ under plane strain condition; E is Young's modulus, v is Poisson's ratio; r and θ are polar coordinates centered at the crack tip with $\theta = 0$ corresponding to the crack tip.

ABAQUS/CAE was used for the analysis. The radius of MBL model was taken as 1000 mm to ensure that the small-scale yielding condition is fulfilled. The model was meshed by standard eight-node elements with reduced integration, CPE8R, with a finer mesh in the crack-tip region and the interface between the weld metal and base metal. The finite element model has 1408 elements and the meshes are shown in Fig.2.

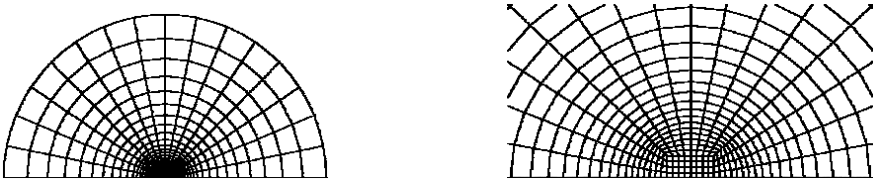

(a) (b)

Fig.2 Modified boundary layer model, (a) global mesh; (b) crack-tip mesh.

The base metal and the weld were assumed to have the same elastic properties (E =2×10^5 MPa, $\upsilon = 0.3$) and the plastic properties but different thermal expansion coefficients. Rate-dependent power law strain hardening materials were used, which have the form of

$$\sigma_f = \sigma_0 \left(1 + \frac{\bar{\varepsilon}^p}{\varepsilon_0} \right)^n \tag{2}$$

where σ_f is the flow stress; $\bar{\varepsilon}^p$ is the equivalent plastic strain, $\sigma_0 = 400$ MPa the yield stress, $\varepsilon_0 = \sigma_0 / E$ the yield strain and n is the plastic strain hardening exponent.

The residual stress field was introduced into the model by so-called eigenstrain method that was also called "inherent strain" method when first introduced by Ueda [9]. The basic idea of eigenstrain method is that the source of residual stress is an incompatible strain field caused by plastic deformation, thermal strains and phase-transformation etc. [10]. Thus, if the distribution of the eigenstrain is known, the distribution of residual stresses can be obtained through linear elastic calculation by using the finite element method. In this study, the isotropic distribution of eigenstrain in both the base metal and weld metal regions was assumed. The eigenstrain values were set to be equal to the thermal expansion coefficients of two regions (α_w and α_b), respectively. The residual stresses were then introduced by loading the model with a unit temperature change. Fig.3 presents the redistributed residual stress after the crack was introduced for the case with eigenstrain $\alpha_w = 0.003$ and $\alpha_b = 0$. The stress components were normalized by the yield stress, and the distance from the crack tip was normalized by the radius of the weld metal region c.

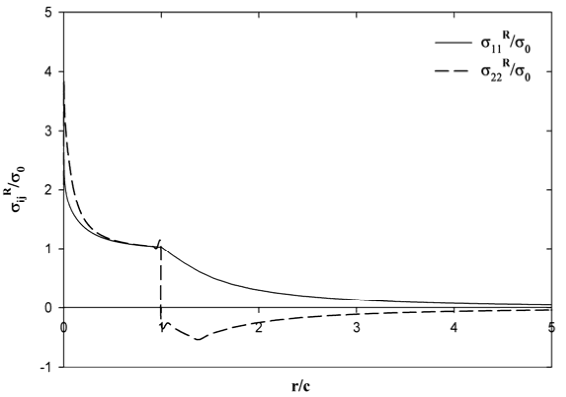

Fig.3. Residual stress field introduced by the eigenstrain method. E/σ_0 =500, υ =0.3; n=0.1; α_w =0.003, $\alpha_b = 0$; c=20mm .

It can be seen that the residual stresses along both the parallel and opening directions have a sharp turning point at the interface of the base metal and weld metal. The reason for the sharp turning point is that the assumption of the eigenstrain distribution is not continuous between the two regions. It can also be seen that both the parallel and opening residual stresses in the weld metal are tensile. In the base metal region, the residual stress parallel to the crack plane is also tensile in a large range while the opening residual stress is compressive to counter balance the tensile stress in the weld.

Results and discussion

J-integral [11] is adopted by the majority of the integrity assessment procedures currently used as the elastic-plastic fracture parameter. In this study, the computed *J-integral* by ABAQUS has been investigated. It was found that the *J-integral* in both the cases with and without residual stress loses path independence in the finite-strain region, beyond which the *J-integral* are practically path-independent. The calculated *J-integral* has been used in the calculation of the stress field. *J* in following means the calculated *J-integral*.

The reference solution is important for studying the crack-tip constraint. The stress field distribution according to the HRR [12, 13] singularity or the small scale yielding solution (SSY) from MBL analysis can be used as the reference field. The difference between the HRR singularity and SSY solution was found to be very small. Dodds et al. [14] showed that the choice of HRR field or SSY solution as reference field does not result in any significant difference. In this study, we used a homogeneous SSY solution without residual stresses and the *T-stress* as the reference field. Small scale yielding conditions are enforced by not allowing the plastic zone r_p to exceed 0.2 times the radius of the MBL model.

Definition of R

In order to quantify the residual stress-induced crack-tip constraint, different residual stress fields were introduced by varying the eigenstrain values under the same external loading controlled by the *K-field*. The stress distributions including the residual stresses are compared with the reference SSY solution in Fig.4. Here, the stress components along the crack line ($\theta = 0$) were shown in the range $0 < r/(J/\sigma_0) < 5$.

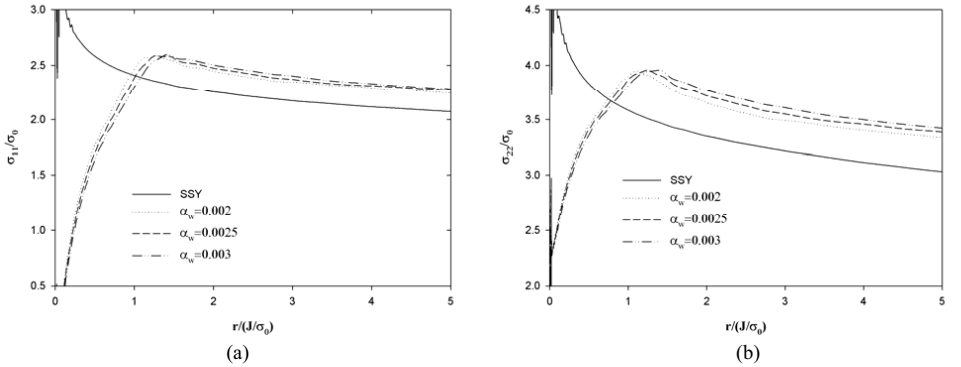

Fig.4. Comparison of the reference field and the stress field including residual stresses along $\theta = 0$, $J_{applied}$=200 N/mm. E/σ_0 =500, υ =0.3; n=0.1. (a) σ_{11}; (b) σ_{22}.

It can be seen that the presence of the residual stresses elevates the stress level significantly compared with the reference solution, and the elevation of the stress level increases with the increase in the eigenstrain level. It can also be observed that that the finite-strain effects are significant in the range $r/(J/\sigma_0) < 1.5$, beyond which the stress distributions seem to be parallel to each other. Due to the symmetrical condition, the shear stress component is zero.

The difference stress field has been calculated between the full stress fields with residual stresses and the reference solution and plotted in Fig.5.

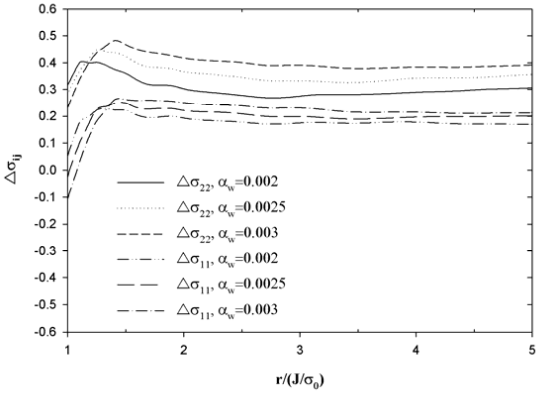

Fig.5. Difference stress between the full stress field and reference solution along $\theta = 0$ with T=0. E/σ_0 =500, υ=0.3; n=0.1.

As shown in Fig.5, $\Delta\sigma_{11}$ and $\Delta\sigma_{22}$ are different for the same eigenstrain level. With the increase in the eigenstrain level, the difference between $\Delta\sigma_{11}$ and $\Delta\sigma_{22}$ increases. However, Liu et al. reported that the residual stress-induced different field could be approximated by a hydrostatic stress field [8]. It should be noted that uniaxial residual stress field perpendicular to the crack flank was used in [8] while biaxial residual stress field was introduced in this study. Thus, the different results in [8] and current study may be explained by the different residual stress fields.

It is known that the cleavage fracture is controlled by the critical levels of the opening stress acting over a microstructurally significant distance ahead of the crack tip. A parameter R was then defined based on the difference in the opening stresses to quantify the residual stress-induced crack-tip constraint. The definition of R is:

$$R = \frac{\sigma_{22} - (\sigma_{22})_{SSY,T=0}}{\sigma_0} \quad \text{at } r = 2J/\sigma_0 \tag{3}$$

Here, the distance $r/(J/\sigma_0) = 2$ is chosen so that R is evaluated outside the finite-strain region. The difference between the finite strain solution with T=0 and reference small scale yielding solution is negligible when the distance is greater than $r/(J/\sigma_0) = 2$.

Effect of external loading on R

The structures with the residual stresses are subject to various service loading conditions. It is interesting to investigate the effect of external loading on the residual stress-induced crack-tip constraint. In this study, a residual stress field with eigenstrain value $a_w = 0.003$ and $\alpha_b = 0$ was introduced into the MBL model, and the residual stress-induced constraint parameter R was

calculated according to Eq.3 under five external loading levels ($J_{applied}$=200,300,400,500 and 600 N/mm), Fig.6.

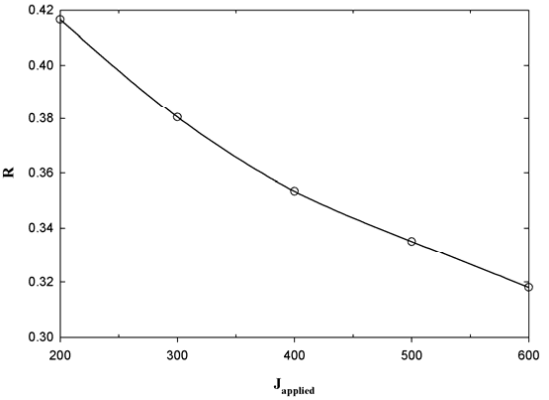

Fig.6. The relationship between *R* and external loading. E/σ_0=500, υ=0.3; *n*=0.1; α_w=0.003, $\alpha_b = 0$.

It can be seen that the residual stress-induced constraint *R* decreases with increase in the external loading. Liu et al. [8] reported a similar trend in their study. The behaviour is in agreement with the common knowledge that the external loading and plasticity can reduce the effect of residual stresses.

Effect of hardening component on R

The material properties can also influence the residual stress-induced crack-tip constraint *R*. In the present study, the residual stress field generated by eigenstrain values $a_w = 0.003$ and $\alpha_b = 0$ was used. The *R* value was calculated according to Eq. 3 and plotted as a function of hardening component in Fig.7.

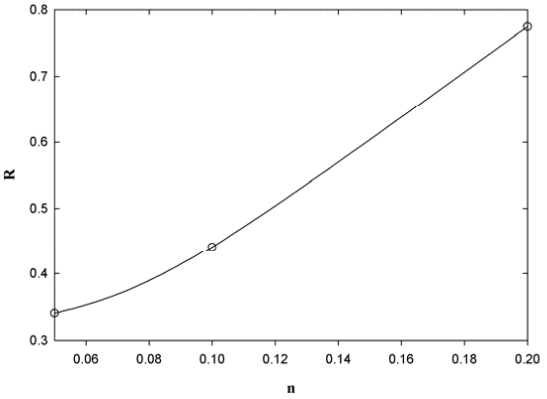

Fig.7. The relationship between *R* and hardening component *n*. E/σ_0=500, υ=0.3; $J_{applied}$=200 N/mm; α_w=0.003, $\alpha_b = 0$.

Fig.7 shows the *R* value increases with the increase in the hardening component *n*, and the effect of residual stresses on the crack-tip constraint becomes smaller for materials with weaker hardening.

Effect of geometry constraint on R

The effect of geometry constraint was also investigated in this study. By changing the *T-stress* in Eq.1, different constraint level can be obtained at the crack-tip. The relationship between *R* and *T-stress* calculated by Eq. (3) is shown in Fig.8.

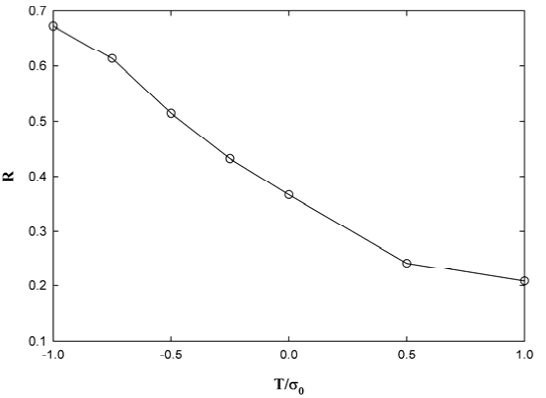

Fig.8. The relationship between *R* and *T-stress*. E/σ_0 =500, υ=0.3; $J_{applied}$ =200 N/mm; α_w=0.003, $\alpha_b = 0$.

It can be seen that *R* decreases with the increase in the *T-stress*. Thus, the effect of residual stress on the crack-tip constraint becomes larger for the lower geometry constraint case. The change of *R* is relatively small when $T/\sigma_0 > 0.5$.

Summary

The residual stresses affect both the crack driving force and the crack-tip constraint. This study focused on the latter effect by defining a new parameter *R*. The parameter *R* was defined based on the difference in opening stress component between the full stress field and the reference field. A two-dimensional residual stress field was introduced into the MBL model by eigenstrain method.

The results show that the residual stresses elevate the stress field significantly compared with the reference field. The *R* value decreases with the increase in external load. The effect of residual stresses on the crack-tip constraint becomes smaller for a stronger hardening material. The result also demonstrates that the effect of residual stresses on the crack-tip constraint is smaller for the case with higher geometry constraint. The residual stress-induced crack-tip constraint also depends on the level of residual stress field itself. Therefore, the constraint parameter *R* can be constructed as:

$$R = F\left(\varepsilon^*, n, Q, P\right) \tag{4}$$

where ε^* represents the eigenstrain; *n* is the hardening component; *Q* measures the geometry constraint; *P* characterizes the external loading.

Acknowledgment

The funding from the Research Council of Norway through the "STORFORSK" project No.167397/V30 is greatly acknowledged.

References

[1] C. Betegón and J.W. Hancock: Journal of Applied Mechanics Vol. 58 (1991), p.104

[2] N. P. O'Dowd and C. F. Shih: Journal of the Mechanics and Physics of Solids Vol. 39 (1991), p.989

[3] N. P. O'Dowd and C. F. Shih: Journal of the Mechanics and Physics of Solids Vol. 40 (1992), p.939

[4] Z.L. Zhang, M. Hauge, and C. Thaulow: International Journal of Fracture Vol. 79 (1996), p.65

[5] C. Betegón and I. Peñuelas: Engineering Fracture Mechanics Vol. 73 (2006), p.1865

[6] M.C. Burstow, I.C. Howard, and R.A. Ainsworth: Journal of the Mechanics and Physics of Solids Vol. 46 (1998), p. 845

[7] P.A. Eikrem, Z. L. Zhang and B. Nyhus: International Journal of Pressure Vessels and Piping Vol. 84 (2007), p. 708

[8] J. Liu, Z.L. Zhang and B. Nyhus: Engineering Fracture Mechanics (2008) doi: 10.1016/j.engfracmech.2008.03.010

[9] Y. Ueda, K. Fukuda, K. Nakacho and S. Endo: Translation of Japan Welding Research Institute Vol. 4 (1975), p.123

[10] M.R. Hill and D.V. Nelson: ASME Pressure Vessels and Piping Vol. 318 (1995), p.343

[11] J.R. Rice: Journal of Applied Mechanics Vol. 35 (1968), p.379

[12] J.W. Hutchinson: Journal of the Mechanics and Physics of Solids Vol. 16 (1968), p.13

[13] J.R. Rice and G.F. Rosengren: Journal of the Mechanics and Physics of Solids Vol. 16 (1968), p.1

[14] R.H. Dodds, Jr., C.F. Shih, and T.L. Anderson: International Journal of Fracture Vol. 64 (1993), p. 101